sustainability

MDPI

Article

The Behavior of a Multi-Story Steel Frame Subject to Measured Fire Using Calibrated Simple Approach

Robin E. Kim [1,*], Xingyue Piao [1] and Jae Hong An [2]

[1] Department of Civil and Environmental Engineering, Hanyang University, Seoul 04763, Korea; seongwol@hanyang.ac.kr

[2] Korea Institute of Civil Engineering and Building Technology, Goyang-Si 10223, Korea; rehong@kict.re.kr

* Correspondence: robinekim@hanyang.ac.kr

Received: 4 September 2019; Accepted: 10 October 2019; Published: 11 October 2019

Abstract: Structural steels are one of the most popular construction materials with a number of merits, such as cost-effectiveness, durability, lightweight, versatility, etc. However, when exposed to a high temperature, their thermal expansion rate is high and the strength reduces substantially, making the steel structures vulnerable to fire. So far, a number of studies have been performed to understand the behavior of steel in fire. Rigorous tests, from the material to structural level, have led the advancement of modeling techniques. Among various analytical techniques, one of the most widely used approaches is the finite element modeling (FEM). While FEM can demonstrate geometrical and material nonlinearities, due to the complexity, the approach may result in high computational loads to ensure the convergence. Thus, in this paper, a simple calculation method is instead used to understand the steel frame subject to fire, in conjunction with experimentally collected temperature and displacement data. Then, at each temperature (before and after critical temperature and the formation of plastic hinges), the effect of elevated temperature on global behavior is examined using frame analysis. Results of the study have demonstrated that when structural integrity is of concern, the critical temperature of the structure must be examined in terms of fundamental characteristics of the structure.

Keywords: critical temperature; elastic analysis; plastic hinge development; simple calculation approach; steel-framed structure; structural fire engineering

1. Introduction

Despite the popularity of steel as constructional materials, steels show degraded performance when exposed to fire. The strength factor of steel reduces to 60% of its original at around 550 °C. Some historical fire disasters such as World Trade Center Tower 1, 2, 5 and 7 in New York and Windsor Building in Madrid, Spain reveal that fire on a steel-framed structure can result in large deformation and total or partial collapse of the structure. Although the structural failure of a steel frame structure solely due to fire is rare [1], understanding the integrity of the steel structure subject to fire is still essential for reducing social losses.

To date, numerous researches have been performed to understand the behavior of the steel structure. Substantial experiments, from small-scale to full-scale, have contributed to the development of modeling techniques. Wainman and Kirby (1998, 1999) [2,3] conducted a standard fire test using unprotected simply supported steel beams to predict different constitutive models. Between 1994 and 1997, Cardington Research Program in Bedfordshire, England performed a series of full-scale tests of a steel-framed structure [4]. The results from the large scale test helped to establish structural fire engineering design methods. Also, empirical results helped to validate the analytical tools,

where widely used tools that can assess the global behavior of the structure can be categorized into two: Finite element methods (FEM) and simple calculation methods [5].

Many researchers have investigated finite element approaches to assess structural behavior under fire [6–9]. FEM is powerful for handling formulations with both material and geometric nonlinearities. To list a few, [10] and [11] proposed nonlinear formulation for predicting the plastic behavior unprotected steel members by accommodating elastoplastic strain hardening. SAFIR, developed by a group of researchers at the University of Liege, Belgium, is also a finite element based program [12]. The program targets to solve structural fire and associated non-linearity by step-by-step simulation. Despite the powerful features of FEM, most software tools are problem-specific, require long computational time when structure gets complicated and may become less flexible when combining with other resources is needed. Thus, especially when a rapid assessment or decision making is required, a simpler tool is beneficial.

Simple calculation methods show great computational power with no iteration process needed in the analysis. Thus, early efforts in the simple calculation methods have been made with the use of empirically obtained formulations. As described in [13], such an approach aims to calculate the load ratio, which is a function of applied bending moment at room temperature, and moment capacity at limiting temperature. Wong (2001) claimed that such an approach may fail to reflect the reality where the static loading and thermal loadings actually interact with the structural members [5]. Instead, in the paper, elastic and plastic methods are proposed to identify a critical member and limiting temperature in a steel structure subject to fire conditions. The presented approach revealed that the elastic method is fairly straightforward and has potential to assess the structural integrity of a low-rise building or subassemblies of a larger structure, and thus will be adopted in this study.

Nevertheless, most of the analysis either uses the standard fire or monotonically increasing temperature, while in reality, the temperature rise is rather a challenge to be measured. Further, as will be described more in the later section of this manuscript, to estimate the temperature gradient of a structure, heat transfer analysis is essential. A group of researchers has used measurement tools such as thermocouples, strain gauges, and also fiber optic sensors to directly obtain the surface temperature [14,15]. Among them, the authors in [16] proposed a framework that estimates thermal loads of a structure to directly apply steel surface temperature to the numerical model, by installing a cluster of temperature sensors on the surface of the steel to be transmitted wirelessly. The developed framework showed the potential of monitoring the integrity of a steel-framed structure during a fire.

Thus, this paper presents a calibrated simple-calculation approach for quickly assessing the stability of a steel-framed structure during a fire disaster. Sets of measured temperature are collected from the framework described in [16]. Then, a numerical analysis is performed to understand the development of plastic hinges and the critical temperature. The simplicity of the simple calculation approach ensured the fast interpretation of the entire structure during each simulation step. At the same time, using the direct stiffness matrix method, the fundamental characteristics of the structure have been identified. By comparing natural frequencies, the critical scenarios for the described structure have been sought. Results of the study have demonstrated how measured temperature can be directly applied for understanding the structural integrity of the steel frame. Finally, this research aims to further contribute to the realization of real-time monitoring of a structure during a fire.

2. Review of Traditional Structural Analysis on Steel Structures

2.1. Experimental Calibration on FEM Approaches (Hybrid Simulation)

As in the case of fire, where the problem contains material and geometrical nonlinearity, experimental testing is an essential tool for understanding its structural behavior. Although conducting full-scale testing can provide in-depth understanding, due to its challenges in test setup and accompanying large cost, such tests are rare [17].

Alternatively, some researchers investigated hybrid fire simulation. The basis of hybrid simulation is that the structure to be tested is divided into a set of physical models and the remaining numerical

model [18]. In the field of fire engineering, the first hybrid fire simulation was reported by [19], where the researcher conducted tests with a 6-story reinforced concrete building. Later on, several other research groups also reported on hybrid fire simulation. To list a few, groups of researchers can be found in [20].

Among the aforementioned research, the authors in [21,22] proposed and conducted an automated displacement controlled hybrid fire simulation on a full-scale steel specimen subject to high temperature. Using the reference structure described in Figure 1 and section properties listed in Table 1, the middle column on the first floor (element ID #9) was replaced with physical columns in full-scale and tested in a furnace. As the column was exposed to fire, the displacement was enforced to the physical column to satisfy the compatibility and to force equilibrium at each time step. Because the test was conducted for the entire structure, the connection movement (behavior) between the column and the rest of the structure was also stored in the database. In this paper, as a benchmark problem, the datasets from Wang et al. [21,22] are used to develop a methodology for assessing the integrity of the structure.

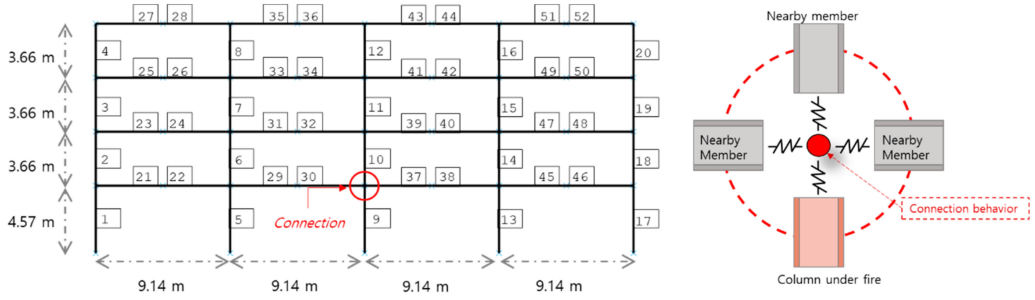

Figure 1. Illustration of problem sets (**a**) Reference structure layout [21,22]; (**b**) Zoomed connection to describe the modeled connection behavior.

Table 1. Section properties of the reference frame [21,22].

Element ID	Section Property	Element ID	Section Property
1, 17	W14 × 233	7, 11, 15	W14 × 176
2, 18	W14 × 193	21, 22, 29, 30, 37, 38, 45, 46	W33 × 130
3, 19	W14 × 099	23, 24, 31, 32, 39, 40, 47, 48	W27 × 114
4, 8, 12, 16, 20,	W14 × 074	25, 26, 33, 34, 41, 42, 49, 50	W27 × 094
5, 6, 10, 13, 14	W14 × 311	27, 28, 35, 56, 43, 44, 51, 52	W24 × 068

2.2. Simple Calculation Approach

A simple calculation approach has great merits over the FEM approach for being able to assess the structural condition under high temperatures quickly. The major difference is that the simple method does not require an iterative solution approach, as in FEM. The author in [5] proposed an elastic method, which can identify the critical member reaching its limiting temperature subject to the fire load. Especially with assumptions that the initial external loads remain constant throughout the procedure, and the bending moment becomes the most critical factor. Then, the limiting condition can be written as below:

$$\phi_T M_e^* + M_L^* - \phi_{yT} M_C = 0 \tag{1}$$

where, M_e^* is the bending moment due to a thermal load, M_L^* is the bending moment derived from the static loads, M_C is the moment capacity of each member within the structure. ϕ_{yT} is a load ratio of yield stress between at a temperature T (f_{yT}) and at room temperature (f_{y20}):

$$\frac{M^*(T)}{M_C} \leq \frac{f_{yT}}{f_{y20}} = \phi_{yT} \tag{2}$$

In addition, elastic modulus ratio, ϕ_T can be described as below:

$$E_T = \phi_T E_{20} \tag{3}$$

where E_{20} is the elastic modulus at 20 °C, and E_T is the elastic modulus at temperature T. Various design codes suggest different expressions for obtaining ϕ_T, while in this paper, the relationship given in AS 4100 [23] and NZS 3404 [24] will be used as a basis. The two-curve approximation has been chosen in the study:

$$\begin{aligned} \phi_T &= 1.0 + T/\left[2000 \ln\left[\tfrac{T}{1100}\right]\right] \quad \text{for } T \le 600\ ^\circ\text{C} \\ &= 690(1 - T/1000)/(T - 53.5) \quad \text{for } 600 < T \le 1000\ ^\circ\text{C} \end{aligned} \tag{4}$$

In summary, to realize the real-time assessment of the structural integrity of a steel-frame subject to fire, temperature needs be first calibrated with experimental results (hybrid simulation described in Section 2.1) in order to understand the connection behavior, and safety of the structure will be assessed through a simple calculation method.

3. Methodology

3.1. Calibration of the Measured Temperature

This section further calibrates ϕ_T using measured specimen displacement to include connection behavior. At a material level, the change of elastic modulus can be described by ϕ_T in Equation (4). However, at a system level, the displacement is also affected by the connected members, which can be considered an actual stiffness of the member.

Thus, from the hybrid simulation conducted in [21,22], specimen displacement and reaction forces are calculated (see Figure 1 for the reference structure and Figure 2 for the full-scale specimen and test setup). Here, because the displacement reading directly obtained from the actuator side contains not only deformations of the specimen but also that of the reaction frame, the displacement of only the specimen has been calculated from the estimated stiffness of the reaction frame. More details regarding the estimation of the specimen's displacement can be found in [21].

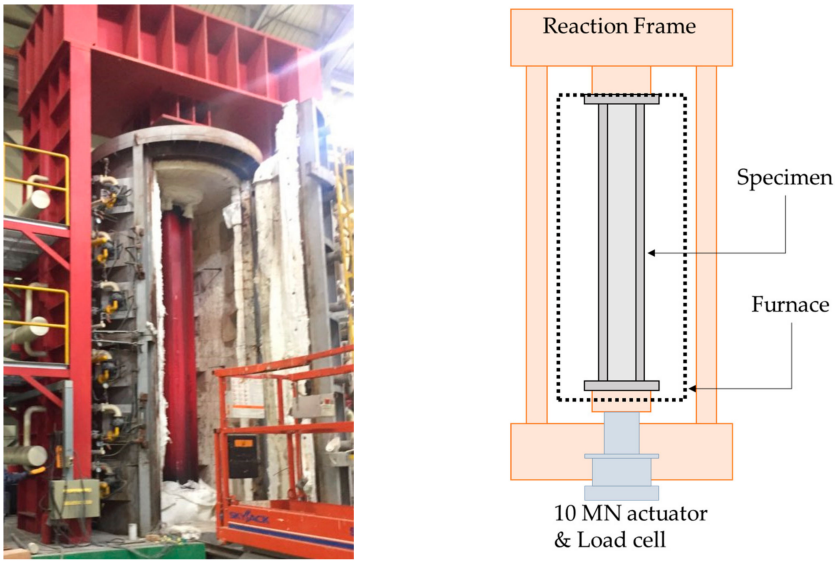

Figure 2. Benchmark experimental setup (**a**) Column furnace and steel column (length of 5 m); (**b**) Schematic description of the test setup.

Based on the direct stiffness method in modeling the frame structure, the initially estimated stiffness matrix ($\left[\boldsymbol{K}_0^e\right]$) is formulated using the material properties at T = 20 °C (E_{20}). The relationships between the external force vector at a time step of t_0 (i.e., $\boldsymbol{P}(t_0)$) and initially estimated displacement vector ($\boldsymbol{u}_0^e$) of the frame is determined.

$$\boldsymbol{P}(t_0) = \left[\boldsymbol{K}_0^e\right]\boldsymbol{u}_0^e \tag{5}$$

Then, at $t_1 = t_0 + \Delta t$, the target elastic modulus $E_{t_1}^T$ is searched such that the estimated displacement of fire exposed member $\boldsymbol{u}_1^e$ calculated from $\left[\boldsymbol{K}_1^e\right]$ and $\boldsymbol{P}(t_1)$ is close to measured column displacement ($\boldsymbol{u}_1^m$) at the same time step. Here, Δt is the time difference between consecutive time steps. Note that a **bold font** implies a matrix, the ***bold italic*** font is used to express a vector, and an *italic font* is used for describing a scalar quantity, i.e.,

$$\text{Minimize } \varepsilon = \left|\boldsymbol{u}_1^e\left|E_{t_1}^T\right| - \boldsymbol{u}_1^m\right| \text{Subject to : } E\left(\boldsymbol{u}_1^e\left(E_{t_1}^T\right)\right) \le E_U\left[\boldsymbol{K}_1^e\right]\boldsymbol{u}_1^e = \boldsymbol{P}(t_1) \tag{6}$$

Note that $E_{t_1}^T$ is applied only to the member that experiences fire and the rest of the members are assumed to be at normal temperature. E_U is the upper bound of the optimization constraint, which is equal to elastic modulus at E_{20}. Such a condition implies that the elastic modulus under fire cannot be larger than its original.

The result from the optimization is described in Figure 3 by comparing the measured displacement and optimized displacement. Note that the measured displacement is obtained during the hybrid fire test in [21,22]. During a hybrid simulation, the temperature of the steel (averaged over the length) was raised up to 733 °C and cooled down, with no global buckle occurring. Although the peak location is slightly delayed, the calibrated results show good agreement while the temperature is being raised. The discrepancy shown in the cool-down phase may have occurred from opening the furnace door: A dramatic change in the temperature could cause the object function to fail to describe the physical phenomenon. Thus, in this study, only the temperature rising phase will be used for the analysis.

Also, the calibrated results (E_t^T) in comparison to a traditional approach (Equation (3)) is shown in Figure 4. The modulus shows a gradually decreasing trend as the temperature rises. Note that the traditional approach showed slightly smaller value when compared with the calibrated results. Especially the difference is larger at the lower temperature, implying that the stiffness of the member could be underestimated under the lower-temperature fire. In the following part of the study, the calibrated elastic modulus result is used for the structural analysis. Note that to be able to describe the failure, which did not occur during the test, E_t^T higher than 733 °C is estimated using the slope at the highest temperature.

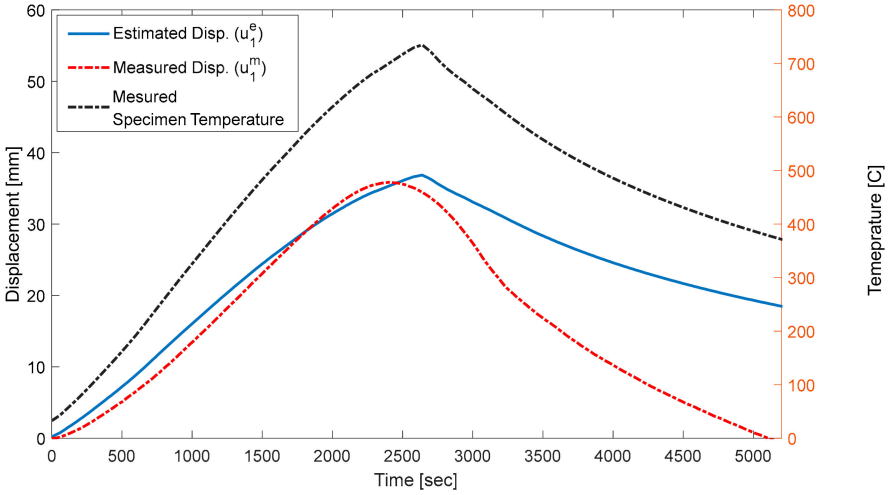

Figure 3. Comparison of column displacement between estimated versus measured data.

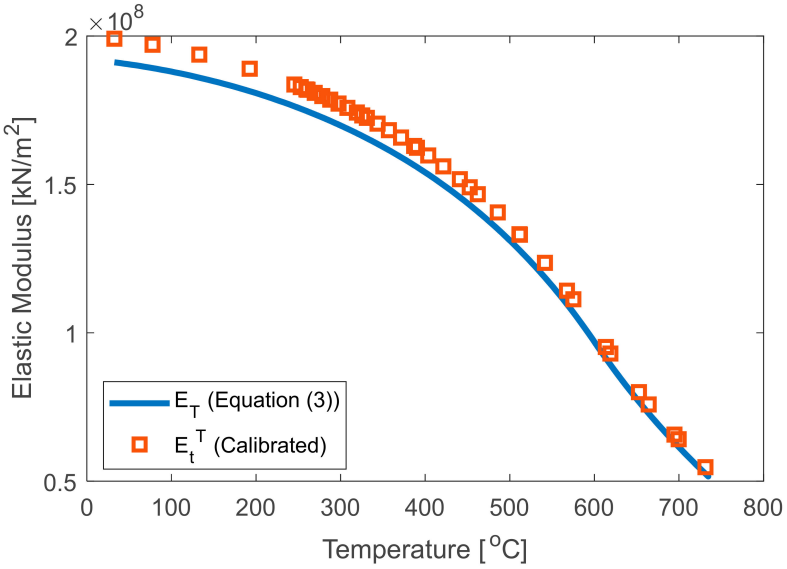

Figure 4. Calibrated elastic modulus.

3.2. Plastic Hinge Propagation Using the Calibrated Simple Calculation Method

In this section, using the calibrated elastic modulus, the propagation of the plastic hinge is examined. Equation (1) is used as the governing equation. First, the initial moment capacity of each element is sought and described in Figure 5. The initial moment capacity beams show larger moment capacity in general, with smaller sections used in the upper story beams.

Then, at every time step as the temperature of the column increases, residual moment capacity (M^*_{Res}) is evaluated:

$$M^*_{Res} = \phi_T M^*_e + M^*_L - \phi_{yT} M_C \quad (7)$$

where, ϕ_T, ϕ_{yT}, and M^*_e are temperature varying quantities. When M^*_{Res} becomes small (near zero) within a member, one can consider that the plastic hinge is developed. Assuming that the initial loads are applied, M^*_L remains constant throughout the analysis. However, when a plastic hinge is developed, to accommodate the moment redistribution, M^*_L is recalculated based on the direct stiffness method. And the temperature at which the plastic hinge occurred is noted as the critical temperature of the member. In this specific problem, the critical temperature occurred at 891 °C.

To further examine how the moment capacity is reached, M^*_{Res} of the fire exposed member is plotted in Figure 6. Up to around 200 °C, the ratio residual stress over the moment capacity remained the unity, implying that the contribution of temperature rise is minor. Also, note that at 733 °C, when the experiment was terminated, the column still had about 20% of residual capacity. This phenomenon approves the fact that the column did not fail during the experiment.

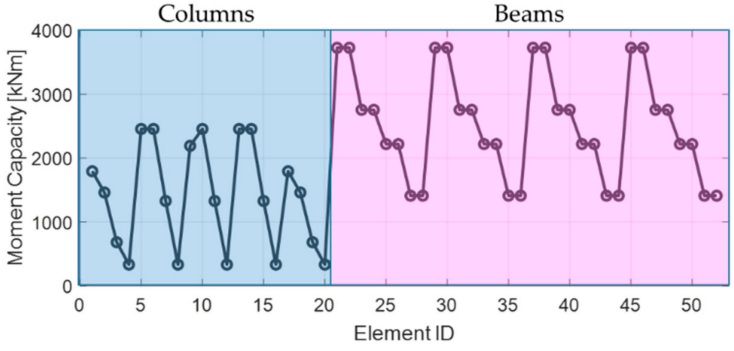

Figure 5. The initial moment capacity (M_c) of each element.

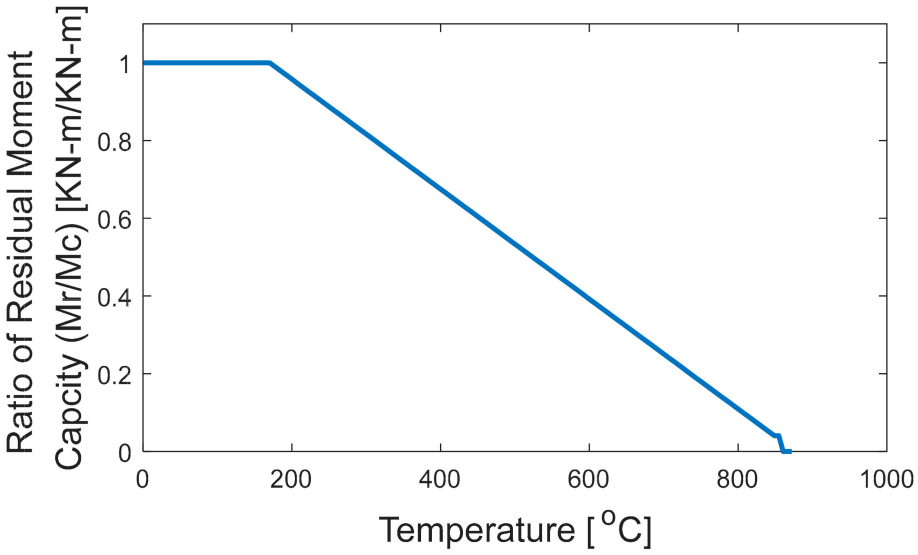

Figure 6. The ratio of residual moment capacity (M_r) of the fire exposed member with respect to initial moment capacity.

3.3. Moment Redistribution Due to Plastic Hinge

After a member reaches its moment capacity, the plastic hinge develops, and no further moment can be carried. Figure 7 compares the moment distribution within the reference frame just before the hinge develops (Figure 7a) and the right after the critical temperature (Figure 7b). The hinge is noted with a red dot in Figure 7b and the moment carried by the column (Element ID #9) has been distributed to other elements. Especially, outer columns and beams seem to carry more moments after the critical temperature. However, the presented analysis assume that the axial load is small such that the load-carrying capacity and the interaction with moment capacity can be neglected. Such an assumption simplifies the calculation process and can be used for validating the analysis.

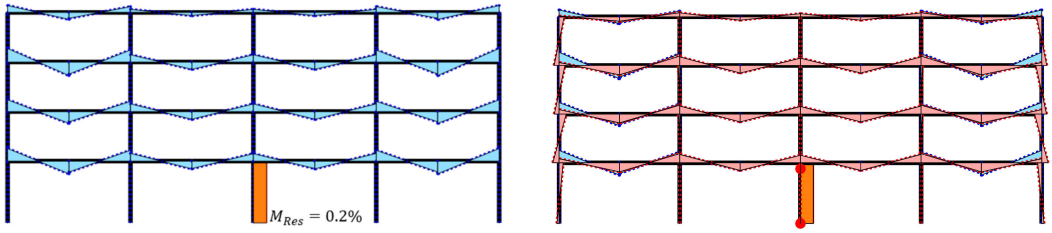

Figure 7. Moment diagram within the reference frame (**a**) Before the critical temperature; (**b**) After the critical temperature.

4. Case Study and Fundamental Characteristics of the Structure

In this section, to present a more realistic phenomenon, a beam, which the bending governs the formation of plastic hinges, is considered in the analysis. Here, a beam located on the first floor and the second from the left (Element ID 29 and 30 in Figure 1) is assumed to be subject to a fire. The fire load profile and the initial load used in the analysis remained the same as in the previous example.

The critical temperature of the structure is sought until at least a member reaches its moment capacity. At the temperature of 887 °C, the first plastic hinge occurred at the mid-span of the fire exposed beam. The location of the hinge is depicted in Figure 8, along with the moment diagram of the frame. A clearer comparison of the moment diagram before and after the critical temperature is shown in Figure 9. Note that each element contains two end moment values, while the plot only compares one end (left-end for the beam and the lower-end for the column). Due to the plastic hinge, the moment

carried by the beam has been redistributed. Nearby beams (Element ID #22 and #37) and columns (Element ID #5, #6, #9, and #10) are affected mostly. At the same time, the positive moments carried by exterior beams are also redistributed to the connected columns. The presented results illustrate that the development of a plastic hinge in a local manner can result in the moment redistribution in a global manner.

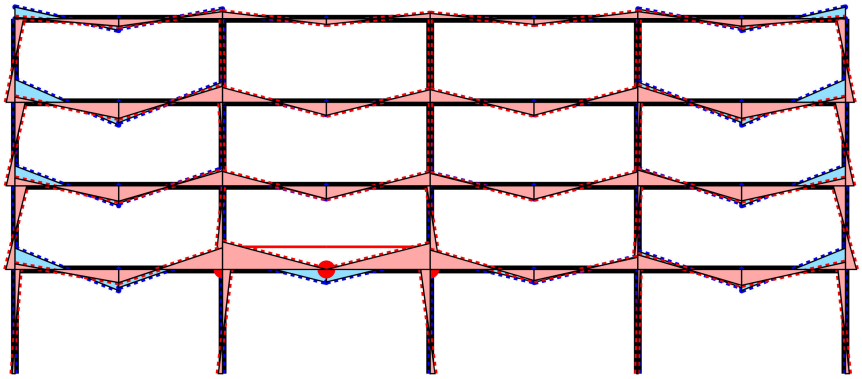

Figure 8. Moment diagram within the reference frame case II.

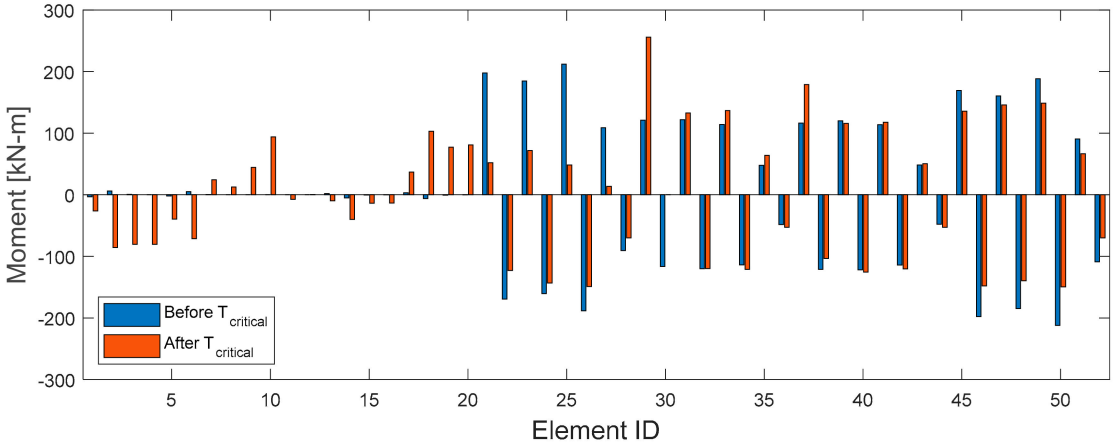

Figure 9. Comparison of the member-end moment of the structure.

Now, to further examine the effect of change in material property due to elevated temperature and the development of a plastic hinge, the fundamental frequencies of the structure are found. Figure 10 shows the first six mode-shapes of the building. The first three mode shapes represent the pure lateral modes of the structure, with some local modes mixed in the higher frequencies. In this paper, those first six modes are used for the comparison: This is because that the modes higher than sixth become more local in nature, and the contribution of the higher modes to the dynamic response is usually smaller than that is for the lower modes [25]. At each temperature, the fundamental frequencies are estimated, and their relative changes are plotted in Figure 11. The sixth mode, which is the highest among the group, showed rapid change even at the temperature as low as 100 °C. This phenomenon indicates that the local mode is susceptible to a small change in the material property. Regarding the pure lateral modes, a gradual decrease of those frequencies is captured. About 2% of the difference is captured for the first frequency, while the second and the third frequencies showed very little change (less than 0.5%). The change rate in the fourth frequency is similar to the second mode up to 780 °C, with a drop shown afterward. With the value remaining unchanged after the drop, the critical temperature of the fourth mode may be at 820 °C.

The presented results reveal that the effect of material property change on the mode varies by each frequency and the critical temperature can be different by each mode. Note that the study was being made for the elevated temperature, while the post-fire analysis needs to be performed as well.

Steel usually recovers its material property if not yielded with some residual stresses remained. Thus, the future study that identifies the fundamental modes considering residual stress after a fire is needed.

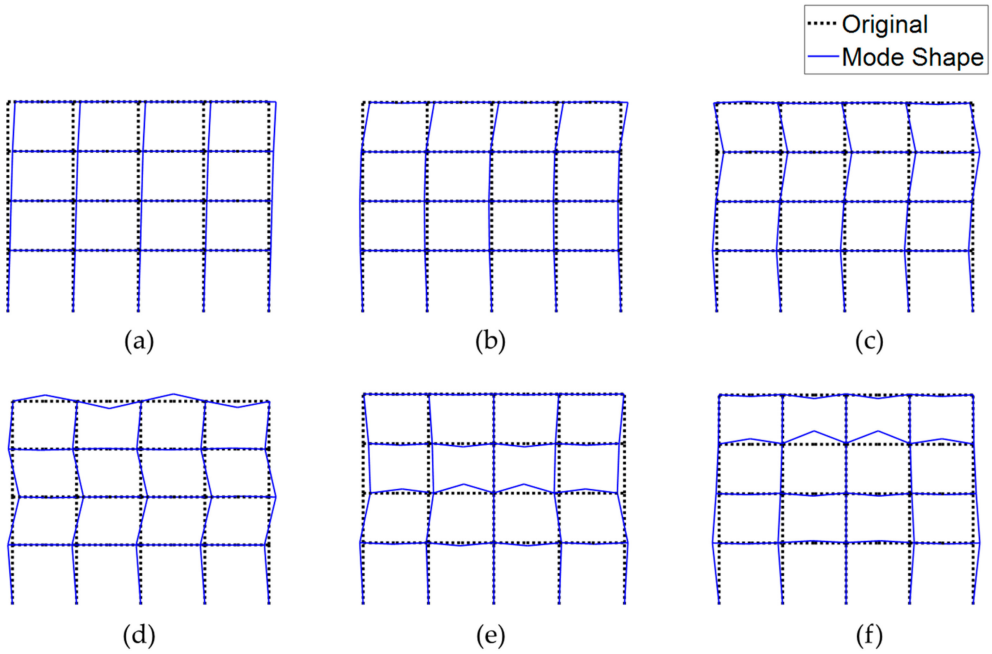

Figure 10. Initial fundamental mode shapes (**a**) 1st lateral mode; (**b**) 2nd lateral mode; (**c**) 3rd lateral mode; (**d**) 4th mode (mixed); (**e**) 5th mode (mixed); (**f**) 6th mode (mixed).

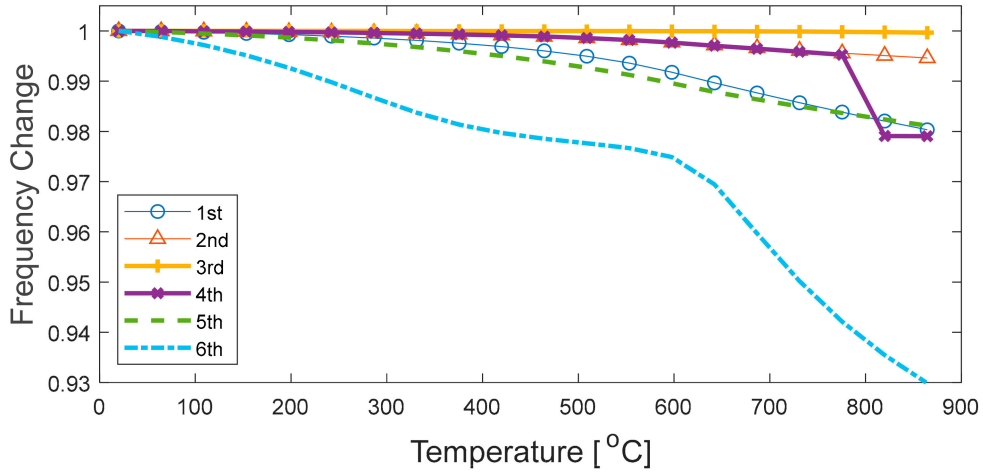

Figure 11. Changes of fundamental mode shape due to temperature rise.

5. Conclusions

A fire on a steel structure can degrade the integrity of the structure, resulting in severe damage. Thus, the presented modeling approach and methodology aims to develop a rapid tool that can assess the plastic development of a steel structure and the changes in the fundamental characteristics subject to a fire. Having a four-story frame structure as a reference building, the connection behavior within the structure subject to fire is obtained from prior research. The stiffness of the structure has been calibrated using the measured data with an optimization process and obtained a generalized connection behavior. When compared with the traditional approach, the calibration of the stiffness results in slightly larger elastic modulus, which otherwise would have been underestimated. Then, assuming that the moment is the major cause of the plastic hinge formation and also that the interaction between the axial force capacity is small, a simple calculation method has been applied to the structure. Once the critical temperature is identified, the moment diagram of the structure before and after the plastic hinge

formation has been compared. The redistributed moment showed that the exterior beams can carry positive moment even when those are yet affected by the temperature. Because the aforementioned processes are completed using simple approach, the required no iteration process. Finally, using the direct stiffness matrix for the frame structure the global behavior of the structure has been examined. At each temperature, the fundamental frequencies and mode shapes are calculated, where those quantities are critical for understanding the integrity of the structure. The comparison between the no-fire condition and during fire condition structure showed that the contribution of temperature on the frequency change may vary by each mode, implying that the critical temperature must be examined by the fundamental frequencies. Due to the ease of calculation, the presented tool shows great potentials on being used for near real-time understanding of the fundamental characteristics under multi-disaster, such as earthquake followed by fire. The developed tool can also be used for understanding the structural integrity after a fire to accommodate the residual stress of the structure.

Author Contributions: Conceptualization, R.E.K.; methodology, R.E.K.; software, R.E.K.; validation, R.E.K.; formal analysis, X.P.; investigation, X.P.; project administration, J.H.A.; funding acquisition, R.E.K. and J.H.A.

Funding: This work was partially supported by the research fund of Hanyang University (HY-2019) and by "Development of key technologies for fire forensic investigation of concrete structures, leading to a new paradigm of Underwriting" granted by the Korean government (MSIT) (No. 20190303-001). The authors greatly appreciate the supports.

Conflicts of Interest: The authors declare no conflicts of interest.

References

1. Gewain, R.G.; Iwankiw, N.R.; Alfawakhiri, F. *Facts for Steel Buildings: Fire*; American Institute of Steel Construction: Chicago, IL, USA, 2003.
2. Wainman, D.E.; Kirby, B.R. *Compendium of U.K. Standard Fire Test Data: Unprotected Structural Steel, 1*; British Steel Corporation, Swinden Laboratories: Rotherham, UK, 1988.
3. Wainman, D.E.; Kirby, B.R. *Compendium of U.K. Standard Fire Test Data: Unprotected Structural Steel, 2*; British Steel Corporation, Swinden Laboratories: Rotherham, UK, 1989.
4. Lennon, T. *BRE Cardington Steel Framed Building Fire Tests*; The Building Research Establishment: Inverness, UK, 2016.
5. Wong, M. Elastic and plastic methods for numerical modelling of steel structures subject to fire. *J. Constr. Steel Res.* **2001**, *57*, 1–14. [CrossRef]
6. O'Connor, M.; Martin, D. Behaviour of a multi-storey steel framed building subjected to fire attack. *J. Constr. Steel Res.* **1998**, *1*, 295. [CrossRef]
7. Najjar, S.; Burgess, I. A nonlinear analysis for three-dimensional steel frames in fire conditions. *Eng. Struct.* **1996**, *18*, 77–89. [CrossRef]
8. Saab, H.; Nethercot, D. Modelling steel frame behaviour under fire conditions. *Eng. Struct.* **1991**, *13*, 371–382. [CrossRef]
9. Schleich, J.-B.; Dotreppe, J.-C.; Franssen, J.-M. Numerical simulations of fire resistance tests on steel and composite structural elements or frames. In *Fire Safety Science: Proceedings of the First International Symposium*; CRC Press: Boca Raton, FL, USA, 1986; p. 311.
10. Iu, C.K.; Chan, S.L. A simulation-based large deflection and inelastic analysis of steel frames under fire. *J. Constr. Steel Res.* **2004**, *60*, 1495–1524. [CrossRef]
11. Caldas, R.B.; Fakury, R.H.; Sousa, J.B.M., Jr. Finite element implementation for the analysis of 3D steel and composite frames subjected to fire. *Lat. Am. J. Solids Struct.* **2014**, *11*, 1–18. [CrossRef]
12. Franssen, J.-M. SAFIR: A thermal/structural program for modeling structures under fire. *Eng. J. Am. Inst. Steel Constr. Inc.* **2005**, *42*, 143–158.
13. BSI, British Standard 5950–5958. The structural use of steelwork in buildings. In *Part 8: Code of Practice for Fire Resistant Design*; British Standards Institution: London, UK, 1990.
14. Li, X.; Xu, Z.; Bao, Y.; Cong, Z. Post-fire seismic behavior of two-bay two-story frames with high-performance fiber-reinforced cementitious composite joints. *Eng. Struct.* **2019**, *183*, 150–159. [CrossRef]

15. Bao, Y.; Huang, Y.; Hoehler, M.S.; Chen, G. Review of fiber optic sensors for structural fire engineering. *Sensors* **2019**, *19*, 877. [CrossRef] [PubMed]
16. Kim, R.; In, K.; Yeo, I. Wireless network for assessing temperature load of large-scale structures under fire hazards. *Sensors* **2019**, *19*, 65. [CrossRef] [PubMed]
17. Wang, Y.; Burgess, I.; Wald, F.; Gillie, M. *Performance-Based Fire Engineering of Structures*; CRC Press: Boca Raton, FL, USA, 2012.
18. Carrion, J.E.; Spencer, B.; Phillips, B.M. Real-time hybrid simulation for structural control performance assessment. *Earthq. Eng. Eng. Vib.* **2009**, *8*, 481–492. [CrossRef]
19. Mostafaei, H. Hybrid fire testing for assessing performance of structures in fire—Application. *Fire Saf. J.* **2013**, *56*, 30–38. [CrossRef]
20. Whyte, C.A.; Mackie, K.R.; Stojadinovic, B. Hybrid simulation of thermomechanical structural response. *J. Struct. Eng.* **2016**, *142*, 04015107. [CrossRef]
21. Wang, X.; Kim, R.E.; Kwon, O.-S.; Yeo, I. Hybrid Simulation Method for a Structure Subjected to Fire and Its Application to a Steel Frame. *J. Struct. Eng.* **2018**, *144*, 04018118. [CrossRef]
22. Wang, X.; Kim, R.E.; Kwon, O.-S.; Yeo, I.-H.; Ahn, J.-K. Continuous Real-Time Hybrid Simulation Method for Structures Subject to Fire. *J. Struct. Eng.* **2019**, *145*, 04019152. [CrossRef]
23. Standards Australia. *AS 4100 Steel Structures*; Standards Australia: Sydney, Australia, 1990.
24. Standards New Zealand. *Standards New Zealand, Steel Structures Standard, Part 1*; NZS: Wellington, New Zealand, 1997.
25. Craig, R.R.; Kurdila, A.J. *Fundamentals of Structural Dynamics*; John Wiley & Sons: Hoboken, NJ, USA, 2006.